CHAPTER 11

A comparative study to elucidate the inhibitory mechanism of a 6-mer peptide fragment of $A\beta_{1-42}$ peptide as a potential therapeutic in Alzheimer's disease

A comparative study to elucidate the inhibitory mechanism of a 6-mer peptide fragment of $A\beta_{1-42}$ peptide as a potential therapeutic in Alzheimer's disease

11.1. Abstract:

AD is a neurodegenerative and incurable disease that is associated with the Aβ peptide aggregation. Here, we have carried out comparative MD simulations of a 6-mer peptide and its analogues to elucidate the inhibitory mechanism on Aβ aggregation. The top analogue screened out after refinement via docking exhibited significant inhibitory activities on both $A\beta_{17-42}$ fibril as well as $A\beta_{1-42}$ monomer by leading to disassemble of β-strands of $A\beta_{1-42}$ peptide and fibril by interacting with the C-terminal residues via hydrogen bonds and hydrophobic contacts. Binding of the analogue to the C-terminal region proves to be significant.

11.2. Introduction:

Since $A\beta_{1-42}$ peptide binds to itself with great specificity, $A\beta_{1-42}$ peptide itself can be used as a lead in generating novel fragments that can be modified as inhibitors for the parent peptide. In recent works, many modified peptides derived from the central hydrophobic region of the $A\beta_{1-42}$ peptide sequence have been designed as inhibitors for $A\beta_{1-42}$ peptide aggregation [244-249]. One of the inhibitors which have been modified based on $A\beta_{17-21}$ fragment has completed phase II clinical trials in humans [250]. Similarly, it has been reported that a series of $A\beta_{1-42}$ peptide C-terminal fragments act as the most effective inhibitors of $A\beta_{1-42}$ peptide induced toxicity [251]. Another study has successfully designed N-methylated hexapeptides based on fragment $A\beta_{32-37}$, which proved to be efficient inhibitors of Aβ aggregation [252]. The molecules that possess high binding affinity for the C-terminus of $A\beta_{1-42}$ peptide may disrupt the self-aggregation of Aβ peptide.

Since it is known that hydrophobic interactions play an important role in protein aggregation and also it has been suggested that the hydrophobic C-terminus of $A\beta_{1-42}$ peptide can control its self-aggregation, therefore the designing of inhibitors has shifted to the central hydrophobic sequence of $A\beta_{1-42}$ peptide [253, 254]. Although many laboratories have designed inhibitors to inhibit Aβ assembly based on the C-terminus of $A\beta_{1-42}$ peptide, yet the region remains relatively unexplored. Inhibitors based on C-terminus fragments can easily bind to the parent peptide, and thus may prohibit the

amyloid formation. Bansal and coworkers have reported a number of peptide-based inhibitors that displayed significant Aβ aggregation inhibitory activity [255]. They took the 6-mer $A\beta_{32-37}$ fragment as lead peptide and synthesized 42 new peptides by replacing all the six amino acids by amino acids of both natural and unnatural origin which are isosterically analogous. From the MTT-based cell viability assay, the lead peptide was found to completely protect the cells from $A\beta_{1-42}$ and $A\beta_{1-40}$ peptide induced toxicity and other ten analogous peptides were found to be moderately active on Aβ1-40 induced toxicity. Additionally CD spectroscopy and morphological examination by transmission electron microscopy confirmed the results. However, they have not studied the effect of the analogues on the $A\beta_{1-42}$ induced toxicity. In the present study, we used the lead peptide and the reported analogues of natural origin to study the molecular recognition and inhibitory mechanism using MD simulations.

All the seven analogues of natural origin were assessed via docking to check their binding affinities to $A\beta_{1-42}$ monomer and $A\beta_{17-42}$ fibril relative to the original peptide. We found analogue 6 (IGLMVV) to have higher ACE and surface area relative to the reference peptide. Analogue 6 was therefore used to study for its inhibitory effect on the $A\beta_{17-42}$ fibrils. Furthermore, the top scoring analogue 6 was assessed by performing unbinding MD simulations with the $A\beta_{1-42}$ monomer in explicit solvent subsequently generating their PMF [172] using US [173] simulations. The analogue 6/$A\beta_{1-42}$ monomer complex was first equilibrated in a box of water, and then the analogue 6 was pulled apart at a constant rate, the forces monitored, and the free energy change was calculated as a function of separation. The detailed energetics of the complex formation and the conformational changes underwent by the $A\beta_{1-42}$ monomer was monitored. The revelation of the binding regions of the $A\beta_{1-42}$ monomer with the analogue 6 will be helpful to design more effective inhibitors for $A\beta_{1-42}$ aggregation

11.3. Materials & Methods:

11.3.1. Construction of input files for docking:

i. Computational model of initial $A\beta_{1-42}$ peptide monomer:

The initial $A\beta_{1-42}$ peptide monomer (PDB ID: 1IYT) [211] was retrieved from the RCSB Protein Data Bank [212]. Counter ions (3 Na+) were added to make the net charge of the system zero. TIP3PBOX [170] water model with 10 Å in all directions was used to solvate the system. Total number of particles in the system was 15885.

Further minimization and heating were carried out as described in chapter 5 (section 5.3.1). The conformer with the β-strands generated from the trajectory analysis after 80 ns MD simulation was used for docking.

ii. Computational model of initial reference peptide & the analogues:

The initial reference peptide (IGLMVG) structure was extracted from the $A\beta_{1-42}$ peptide (PDB ID: 1IYT) [211]. The reported seven analogues of natural origin were constructed from the initial reference peptide using Swiss-PDB Viewer [257]. TIP3PBOX [170] water model with 10 Å in all directions was used to solvate the system with reference peptide and analogues individually. A total of 3556 number of water particles were added to the each system. Further minimization and equilibration was carried out as described in chapter 5 (section 5.3.1). The conformers of the reference peptide and the seven analogues representing the most populated clusters after equilibration were used for docking.

iii. Computational model of $A\beta_{17-42}$ fibril structure:

The 2BEG [125] fibril structure was retrieved from the Protein Data Bank [212]. Counter ions (5 Na+) were added to make the net charge of the system zero. TIP3PBOX [170] water model with 10 Å in all directions was used to solvate the initial 2BEG fibril structure. A total of 44,465 water particles were added. Further minimization and equilibration was carried out as described in chapter 5 (section 5.3.1). The conformer representing the most populated clusters after equilibration was used for docking.

11.3.2. Docking of $A\beta_{1-42}$ peptide, $A\beta_{17-42}$ fibril and 6-mer peptide:

The reference peptide (IGLMVG) and the analogues were first assessed by docking in PatchDock server [175] with $A\beta_{1-42}$ monomer and $A\beta_{1-42}$ fibril respectively. The docking result of the reference peptide and the analogues with $A\beta_{1-42}$ monomer and $A\beta_{17-42}$ fibril were calculated. Analogue 6 that resulted in a higher docking score with the maximum atomic contact energy and contact area in comparison to the reference peptide was accepted.

The selected $A\beta_{1-42}$/analogue 6 complex and the $A\beta_{1-42}$/reference complex were solvated in TIP3P water model [170] with a minimum distance of 10 Å to the border and then subjected to a two-step restrained minimization, followed by heating as described in chapter 5 (section 5.3.1). Within the box total number of particles in the system was 16796. Then the individual complexes were equilibrated for 100 ps. As our initial complex structures had attained equilibration, so we ran production MD

simulations for 10 ns. The conformer with the most populated cluster from the last trajectory was used for PMF [172] study as discussed in Chapter 5 (section 5.3.3). The analogue was pulled with a constant velocity along the RC from the receptor peptide $A\beta_{1-42}$.

11.4. Results & Discussions:

11.4.1. Binding characteristics of analogue 6:

Bansal et al., took the 6-mer $A\beta_{32-37}$ fragment as lead peptide and shortlisted ten 6-mer peptides as potent inhibitors of Aβ aggregation after constructing different mutants [255]. In the present study, after docking analysis of the reference peptide and other seven peptides, analogue 6 (IGLMVV) was found to have the highest docking score. The docking result of the analogue with the $A\beta_{1-42}$ monomer and $A\beta_{17-42}$ fibril are shown in **Table 11.1**.

The binding conformations of the analogue 6 with the $A\beta_{1-42}$ monomer and $A\beta_{17-42}$ fibril are shown in **Figure. 11.1. Figure 11.1. A** illustrates $A\beta_{1-42}$ monomer bound to the analogue 6. β-strand in the monomer is shown in green color. The analogue 6 is shown in red color. In **Figure 11.1.B** all the five strands are shown in different colors. This analogue 6 was selected to study the inhibitory mechanism against $A\beta_{1-42}$ peptide aggregation. The analogue 6 was anchored to the amyloid fibril surface by its isoleucine at the N-terminal end. The hydrocarbon side chain of isoleucine fits into the hydrophobic glycine groove where it has hydrophobic interactions. Glycine and Methionine of the analogue 6 also forms hydrophobic interactions with the methionine and closely located valine. Leucine was observed to form direct hydrogen bonds with valine. Their binding characteristics revealed a few key points. It can be concluded that hydrophobic interactions are the primary factor that facilitates analogue 6 binding to the amyloid fibril and the monomer. The secondary factor appears to be the hydrogen bonds.

Table 11.1: *Docking result of the 6-mer peptides with $A\beta_{1-42}$ monomer and $A\beta_{17-42}$ fibril respectively.*

6-mer peptide	6-mer peptide Sequence	6-mer Peptide-$A\beta_{1-42}$ peptide Monomer Complex		6-mer Peptide- $A\beta_{1-42}$ Fibril Complex	
		Area ($Å^2$)	**ACE (kcal/mol)**	**Area ($Å^2$)**	**ACE (kcal/mol)**
Reference peptide	Ile-Gly-Leu-Met-Val-Gly-NH2 (reference peptide)	498.50	-216.23	570.50	-286.81
Analogue 1	Ile-Val-Leu-Met-Val-Gly-NH2	548.20	-310.39	601.50	-342.46
Analogue 2	Ile-Gly-Phe-Met-Val-Gly-NH2	565.90	-277.33	581.70	-267.65
Analogue 3	Ile-Gly-Leu-Met-Pro-Gly-NH2	505.90	-230.51	592.40	-325.67
Analogue 4	Ile-Gly-Leu-Met-Phe-Gly-NH2	535.40	-83.36	563.00	-353.57
Analogue 5	Ile-Gly-Leu-Met-Val-Ile-NH2	540.30	-50.96	611.00	-352.96
Analogue 6	**Ile-Gly-Leu-Met-Val-Val-NH2**	**587.10**	**-305.00**	**600.70**	**-410.23**
Analogue 7	Val-Gly-Leu-Met-Val-Gly-NH2	550.90	-269.53	584.30	-378.35

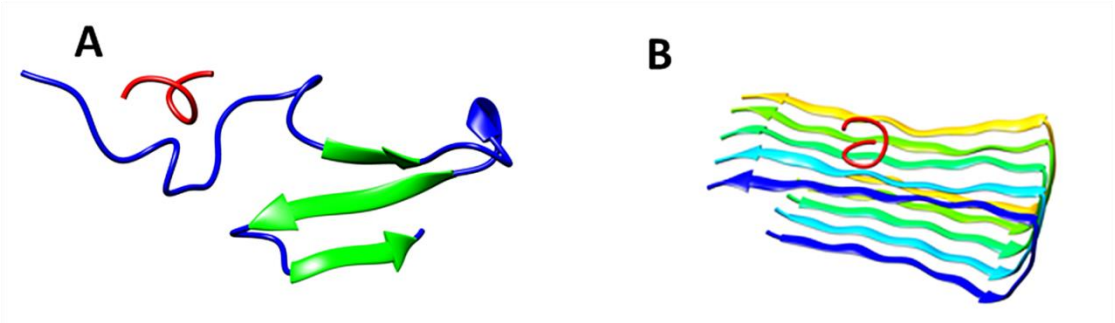

Figure 11.1. *Structure of A) the initial $A\beta_{1-42}$ monomer/analogue 6 complex; B) the initial $A\beta_{17-42}$ fibril/analogue 6 complex with the highest atomic contact energy and surface area score obtained from PatchDock server.*

11.4.2. Effect of the analogue 6 on $A\beta_{17-42}$ fibril:

$A\beta_{1-42}$ peptides that normally adopt α-helix and random coil conformations in aqueous solution undergo transition in their secondary structures to form intra-molecular β-sheet structures under abnormal conditions and aggregates. By MD simulation, we investigated the effect of the analogue 6 on the conformational transition of the $A\beta_{17-42}$ fibril. **Figure 11.2** shows the conformational dynamics of $A\beta_{17-42}$ fibril in presence of the analogue. From **Figure 11.2** we can see the initial complex structure of the $A\beta_{17-42}$ fibril with the analogue 6 bound to it. After 60 ns time interval we notice secondary structural transitions in the $A\beta_{17-42}$ fibril. After 80 ns time interval, we notice disassemble of the β-strands in the fibrils in presence of the analogue 6. Thus in the presence of the analogue 6, the inter-molecular interactions that hold the strands together in the fibril are destabilized, as a result the amyloid fibril undergoes disassembly. The analogue 6 may thus impart its inhibitory effect by destabilizing various interactions and affecting the β-strands in the $A\beta_{17-42}$ fibril. We also ensured the efficiency of analogue 6 as a potent inhibitor from the outcome of control simulation wherein analogue 5 was used (**Figure 11.3**). Moreover, we did not notice disassembly of strands in the fibril structure in absence of 6-mer fragment.

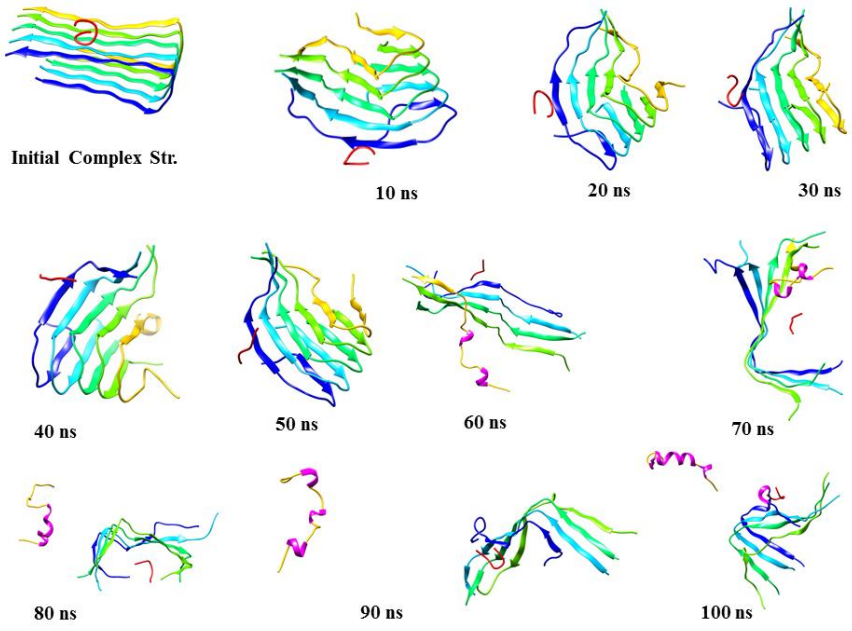

Figure 11.2. *Conformational dynamics of $A\beta_{17-42}$ fibril in presence of analogue 6 at different time course of simulation at 300 K.*

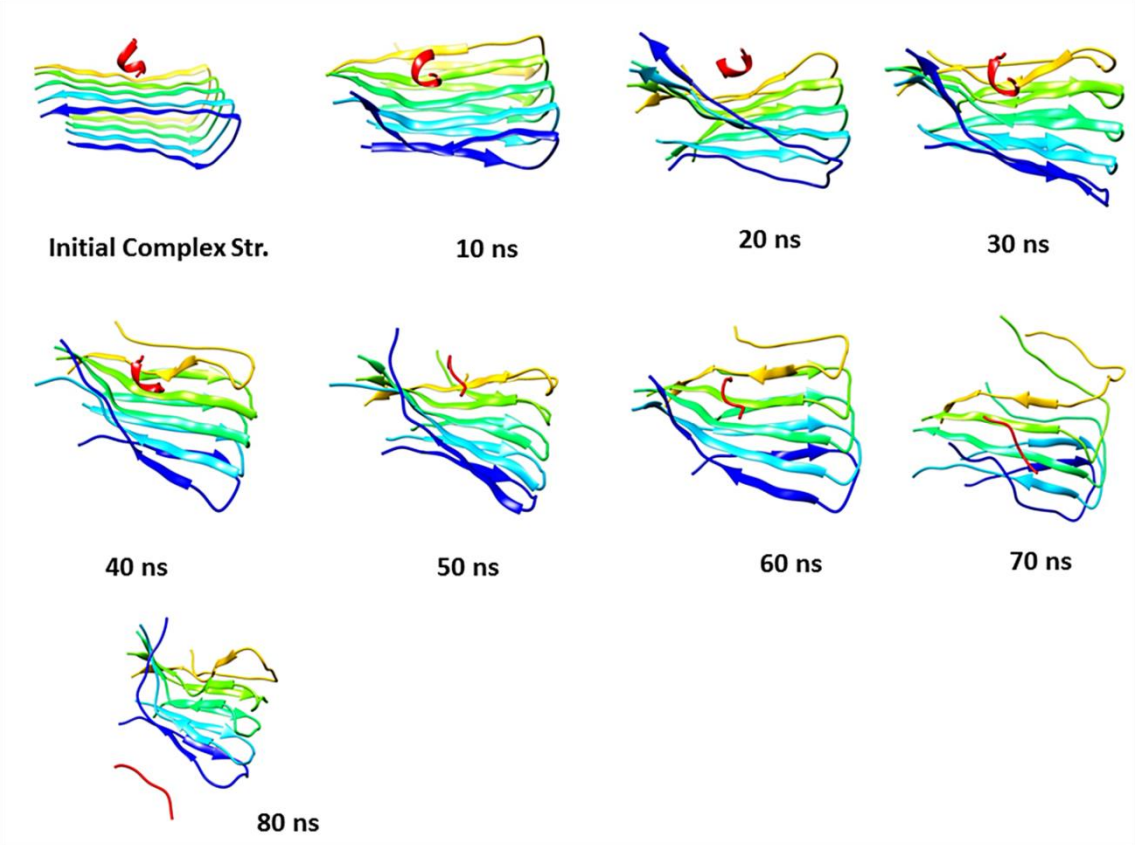

Figure 11.3. *Conformational dynamics of $A\beta_{17-42}$ fibril in presence of analogue 5 at different time course of simulation at 300 K.*

11.4.3. Potential of mean force for unbinding of analogue 6:

We have computed the free energy profile of the association of the reference peptide and the analogue 6 to the $A\beta_{1-42}$ monomer to elucidate their interaction. Thus, the interaction study was performed using US simulations with distance as a function of time whereby the relative binding affinities of the analogue 6 /$A\beta_{1-42}$ monomer complex was determined. **Figure 11.4** shows the result of the free energy profile. The initial reference peptide & analogue 6 /$A\beta_{1-42}$ monomer complex was formed at an inter-chain distance of 11 Å. As we pulled out the reference peptide from the $A\beta_{1-42}$ monomer, we observed a high free energy of ~ 7 kcal/mol. The global minima structure was formed at the inter-chain distance of 11 Å. Thus it can be inferred that the reference peptide binds very strongly with the $A\beta_{1-42}$ monomer.

In case of the analogue 6, as we pulled it out from the $A\beta_{1-42}$ monomer, we observed a low *van der Waals* force of repulsion till a distance of ~16 Å. At a distance of ~16 Å the global minima structure was formed which exhibited the minimum energy

among all the other conformations. After the formation of the global minima structure, the *van der Waals* force of attraction suddenly increased and their dissociation energy was found to be quite high of around 4 kcal/mol.

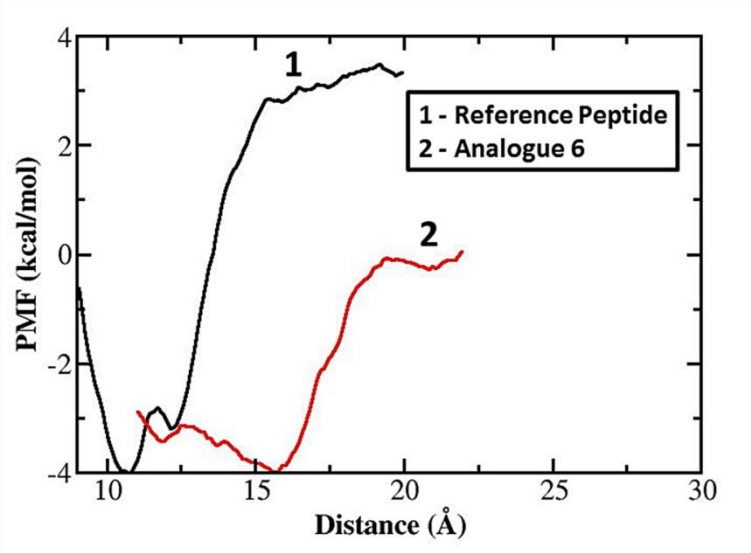

Figure 11.4. *Potential of mean force of $A\beta_{1\text{-}42}$ monomer/reference peptide and $A\beta_{1\text{-}42}$ monomer/analogue 6 (in kcal/mol) as a function of the inter-chain distance (in Å).*

Although the reference peptide was found to bind strongly to $A\beta_{1\text{-}42}$ peptide as compared to analogue 6, the disappearance of β-strands in $A\beta_{1\text{-}42}$ peptide were more prominent in the presence of analogue 6 (can be seen from **Figure 11.5**) than in the presence of reference peptide as shown in **Figure 11.6**. In addition we observed the reference peptide to bind to the N-terminal region of the $A\beta_{1\text{-}42}$ peptide while analogue 6 bind to the C-terminal region of the $A\beta_{1\text{-}42}$ peptide (**Figure 11.5**). As C-terminal region is crucial for $A\beta_{1\text{-}42}$ peptide aggregation, binding of the analogue 6 to the C-terminal region of $A\beta_{1\text{-}42}$ peptide proves to be significant. Additionally, to study the binding characteristics of the reference peptide and the analogue 6 with the $A\beta_{1\text{–}42}$ monomer, we isolated the global minima structures from the free energy profile and carried out analysis for the residue-residue contacts between the reference peptide and $A\beta_{1\text{–}42}$ monomer as well as analogue 6 and $A\beta_{1\text{–}42}$ monomer.

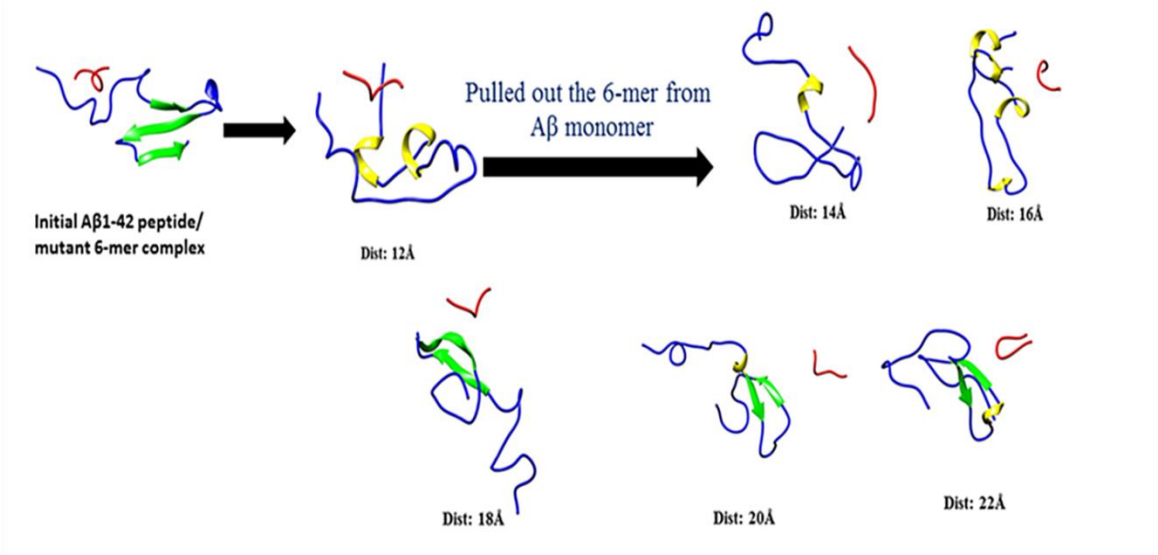

Figure 11.5. *Snapshots of $A\beta_{1-42}$ monomer/analogue 6 complex at different inter-chain distances during the potential of mean force analysis at 300 K.*

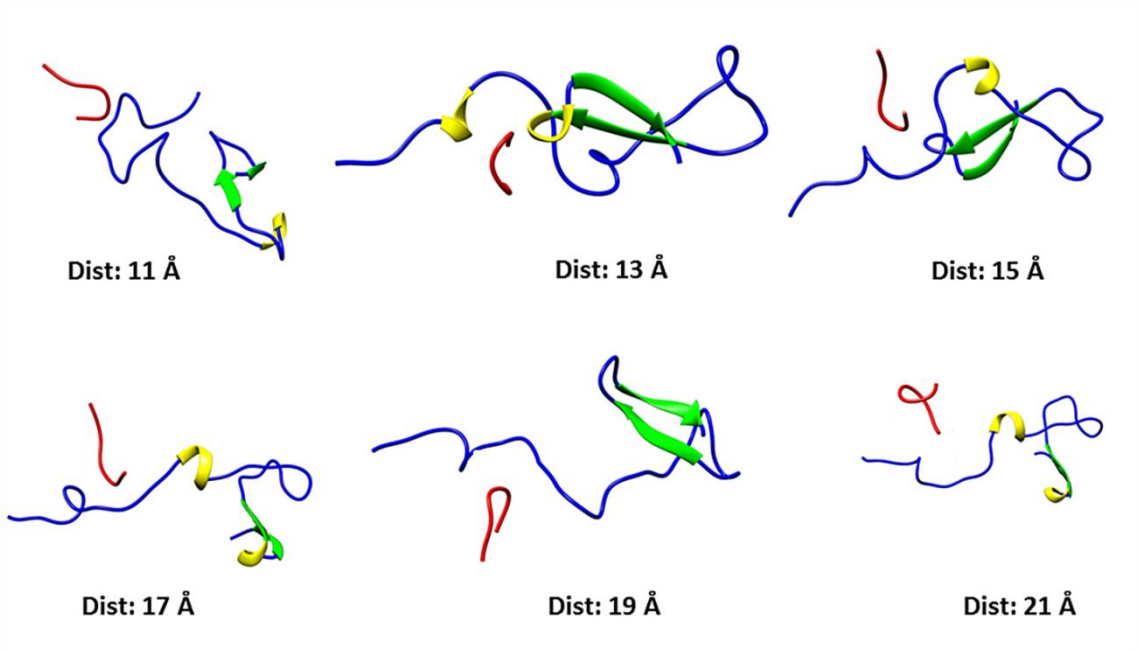

Figure 11.6. *Snapshots of $A\beta_{1-42}$ monomer/reference peptide complex at different inter-chain distances during the potential of mean force analysis at 300 K.*

11.4.4. Binding characteristics of analogue 6 with the $A\beta_{1-42}$ monomer:

In order to study the binding characteristics of the reference peptide and the analogue 6 with the $A\beta_{1-42}$ monomer, we isolated the global minima structures from the free energy profile and examined their interaction profile. The contacts between the residues of $A\beta_{1-42}$ peptide and the reference peptide as well as the analogue 6 were studied based on their shape and chemical complementarity using CMA [178]. The analysis result displays atom to atom contacts for the pair of amino acid residues involved in the interaction in the form of contact map (**Figure 11.7**).

Figure 11.7.A. & B. displays the residues of $A\beta_{1-42}$ monomer that interact with the reference peptide as well as the analogue 6, respectively. From **Figure 11.7.A** we can observe that most of the N-terminal residues of $A\beta_{1-42}$ monomer interact with the reference peptide. Since it is known that the C-terminal region is important for the aggregation of $A\beta_{1-42}$ peptide, binding of the reference peptide to the N-terminal region of $A\beta_{1-42}$ monomer does not seem to be crucial. On contrast, from **Figure 11.7. B** we can observe that most of the residues involved in the interaction between $A\beta_{1-42}$ monomer and the analogue 6 belongs to the C-terminal region and are hydrophobic in nature. Since it is known that the C-terminal region plays an important role in the aggregation of $A\beta_{1-42}$ peptide, binding of the analogue 6 to the C-terminal region of $A\beta_{1-42}$ monomer seems to be crucial.

Furthermore, we have carried out the protein ligand interaction study using PDBSum server [180]. The LigPlot results displaying $A\beta_{1-42}$ monomer-reference peptide interactions and $A\beta_{1-42}$ monomer-analogue 6 interactions are shown in **Figure 11.8.A & B.** respectively. From **Figure 11.8.A & B,** we can observe the hydrophobic interactions as well as hydrogen bonding to be the prime factor to govern the stability of the complex. Arg5, Tyr10, Glu11 and Lys16 of $A\beta_{1-42}$ monomer forms hydrogen bond with the reference peptide; His6, Ser8, Val12 and Leu34 form the hydrophobic interaction (**Figure 11.8.A**). In case with the analogue 6, Ser26, Asn27, Ile31, Val40, Ile41 of $A\beta_{1-42}$ monomer forms the hydrophobic interactions (**Figure 11.8.B**). Lysine and Glycine at position 28 and 29, respectively form the hydrogen bonding with the analogue 6. As we can see from the above results that the analogue 6 binds to $A\beta_{1-42}$ monomer mostly in the C-terminal end which is known to be the aggregation prone

area, we can expect this analogue 6 to be a potent inhibitor of $A\beta_{1-42}$ peptide aggregation.

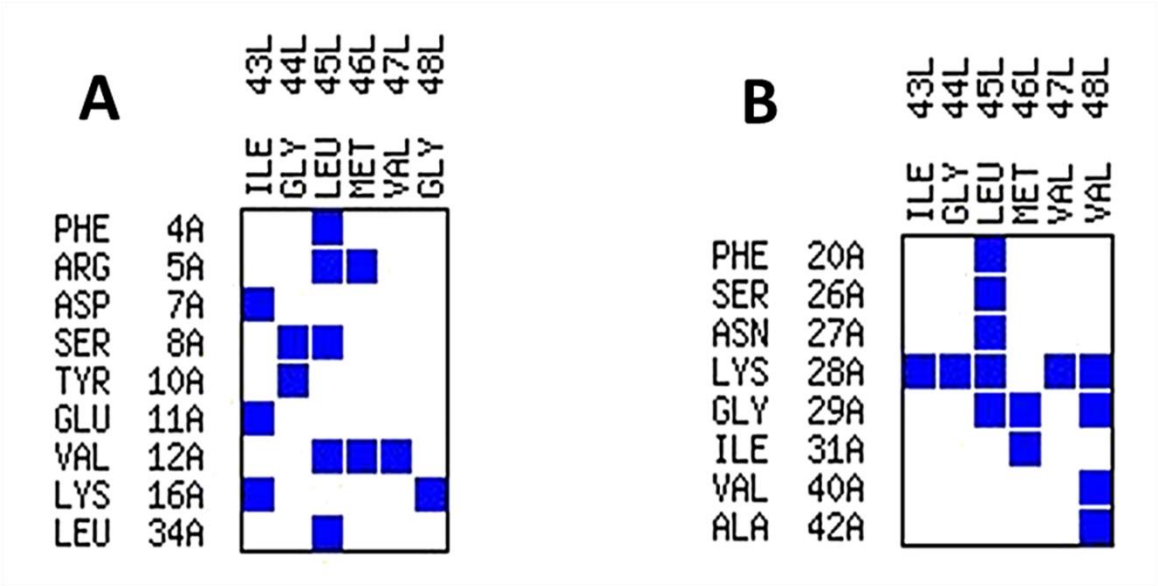

Figure 11.7. *Contact map analysis showing residue-residue interactions in the global minima structure of: A) $A\beta_{1-42}$ monomer/reference peptide complex; B) $A\beta_{1-42}$ monomer/analogue 6 complex.*

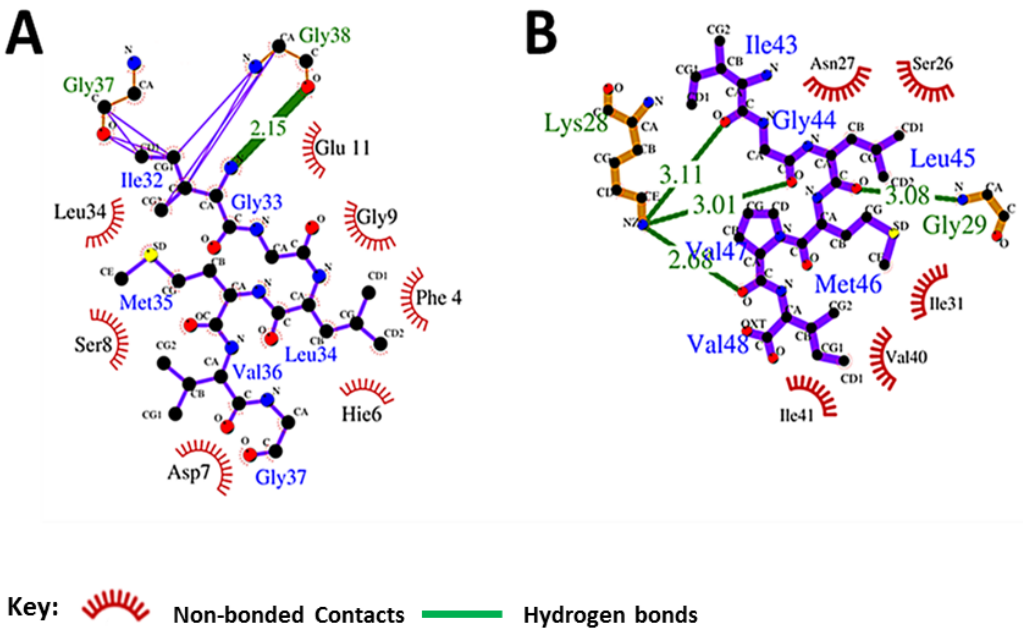

Figure 11.8. *LigPlot analysis showing the interactions as predicted by the PDBSum server of the global minima structure of: A) $A\beta_{1-42}$ monomer/reference peptide complex; B) $A\beta_{1-42}$ monomer/analogue 6 complex.*

11.5. Conclusions:

In this study, we have carried out a comparative study using docking and MD simulations to elucidate the inhibitory mechanism of a 6-mer peptide on $A\beta_{1-42}$ peptide aggregation. Our results indicated one of the analogues to be a potent therapeutic candidate for $A\beta_{1-42}$ peptide aggregation than the reference peptide. Our analogue shows promising results, gives insight to the inhibitor binding mechanism in details, thus giving a direction for further drug designing analysis. The MD simulation of the analogue and fibril complex showed that the analogue binds to the fibril with a high affinity and thus imparts it inhibitory effect by dissociating the fibril to single strands. Also it influences the secondary structural changes in the fibril as well as the monomer by decreasing the β-strand content. From the free energy analysis with the monomer the affinity of the analogue could be confirmed to be strong. High dissociation energy specifies the strong affinity of the analogue to the peptide. Hydrophobic interaction plays an important role in the inhibitory mechanism of the analogue. Formation of strong hydrophobic interaction between the fibril as well as with the monomer leads to the dissociation of the fibril and loss of β-strands respectively. Although the free energy for the reference peptide was higher than the analogue, from the contact map analysis it was found out that most of the residues of the $A\beta_{1-42}$ monomer interacting with the reference peptide were from the N-terminal region. As C-terminal region is crucial for $A\beta_{1-42}$ peptide-$A\beta_{1-42}$ peptide interaction, binding of the analogue to the C-terminal region of $A\beta_{1-42}$ peptide proves to be significant. In the light of the docking and the free energy results, we suggest the analogue to be a potent therapeutic agent.